Geochemical compositional mapping of Lower Jurassic trace fossils: palaeoenvironmental significance and methodological implications

Reolid, J., Reolid, M.

Highlights

XRF compositional maps show geochemical differences between burrows and host sediment

BSE images show relatively high content of pyrite and organic matter within burrows

Environmental conditions for preserving OM were better within burrow galleries

Burrow-water reducing conditions acted as traps for organic matter preservation

Compositional maps are useful for testing geochemical heterogeneity in bioturbated rocks

Geochemical compositional mapping of Lower Jurassic trace fossils: palaeoenvironmental significance and methodological implications

Reolid, Jesús[a]; Reolid, Matías[b*]

[a]*Departamento de Estratigrafía y Paleontología, Universidad de Granada, Spain.* email: jreolid@ugr.es

[b]*Departamento de Geología, Universidad de Jaén, Spain.* email: mreolid@ujaen.es

* Corresponding author

ABSTRACT

Analyses of X-ray microfluorescence (XRF) elemental maps of the ichnofossil assemblages from the upper Pliensbachian-lower Toarcian marl-limestone rhythmite of the South Iberian Palaeomargin (Betic Cordillera, SE Spain) show that the compositions of burrow infills are geochemically and mineralogically different with respect to the surrounding sediment. XRF elemental maps and back-scattered electron images show pyrite framboids within the burrows and enrichment in Fe and S relative to the host sediment. This is congruent with the position of burrows beneath the redox boundary at the time of their active or passive sedimentary infilling. Organic matter that accumulated at the seafloor was not preserved due to oxidation and consumption by benthic organisms. However, burrows located beneath the redox boundary served as traps for organic matter preservation. The composition of burrow fills reflects the original signal of the redox conditions of pore-waters below the sediment-water interface, which was not preserved in the surrounding sediment. The XRF elemental maps also show that some trace fossils

from limestone and marly-limestone intervals contain high concentrations of Si, Al, K, Zn, Cr, and Ti with respect to the surrounding sediment. This may reflect enrichment of clay minerals in the burrow fills derived from overlying marly layers. This work proposes the use of elemental imaging of trace fossils prior bulk-rock geochemical analyses in order to evaluate the potential for biogenic heterogeneity and elemental partitioning before sampling. Geochemical analysis of trace fossils represents an additional tool that may be of use in hydrocarbon exploration.

KEYWORDS: Organic matter; redox conditions; X-ray fluorescence; Pliensbachian;Toarcian; ichnofossil

1. Introduction

It is widely known that burrows may be characterised by redox-related microenvironmental conditions that differ from those at the seafloor (Kristensen, 2000; Wetzel, 2010; Wetzel and Uchman, 2012; Gilbert et al., 2016), which can affect bacterial communities and metabolism (Waslenchuk et al., 1983; Gibert et al., 2016). Sediments infilling burrows may be deposited under different environmental conditions than those at the sediment-water interface. In addition, most tracemakers live in oxic bottom-water and sediments with oxic pore-waters, but some tracemakers are tolerant of low pore-water oxygen levels. These include the tracemakers of *Chondrites*, interpreted to live at the aerobic-anoxic interface as a chemosymbiotic organism (Ekdale and Bromley, 1984; Seilacher, 1990; Fu, 1991), and *Trichichnus* (McBride and Picard, 1991). Moreover, the burrowers can modify redox conditions within the sediment and control the mobility of redox-sensitive elements (Kristensen, 2000; Harazim et al., 2015).

51 The different conditions between sediment infilling the burrow and the
52 surrounding sediment favour the recognition of burrows in sediments when they clearly
53 contrast with the host sediment. Different conditions within burrows are evidenced in the
54 fossil record by different textures, grain sizes, organic matter (OM) contents, and colours
55 of burrow fills compared to that of host sediment. Taphonomy must be considered
56 because erosion, compaction, and diverse diagenetic factors may have significant impacts
57 on the material preserved in the trace fossils (Hallam, 1975). Additionally, the role of the
58 bioturbation and early diagenesis in the origin of nodularity from condensed sections has
59 been widely studied (e.g. Fürsich, 1973, 1979; Eller, 1981; Reolid et al., 2015).
60 Ichnofabrics provide information on palaeoecological and depositional conditions during
61 sedimentation such as oxygenation, sedimentation rate, type of ground, and availability
62 of trophic resources. The sediment pore-water oxygenation is one of the parameters that
63 strongly controls the infaunal assemblages and the ichnofabrics in mud substrates (e.g.
64 Savrda, 2007). Ichnology has proven to be a useful tool for palaeoenvironmental
65 interpretations, basin analysis, and even reservoir characterization (Knaust, 1998; Buatois
66 and Mángano, 2011; Ekdale et al., 2012; Giraldo-Villegas et al., 2016; Rodríguez-Tovar
67 et al., 2017, Reolid and Betzler, 2019). Some studies have attempted to connect
68 ichnological attributes to geophysical and geochemical proxies such as the natural gamma
69 radiation (Reolid and Betzler, 2018; Reolid et al., 2019a). However, systematic analyses
70 of the geochemical composition of trace fossils and host rocks from marls and marly
71 limestones are scarce (Izumi, 2013; Izumi et al., 2014; Harazim et al., 2015).
72 The aim of this work is to use X-ray microfluorescence elemental maps in order
73 to recognise geochemical differences between trace fossils and their host sediments and
74 to assess their significance in palaeoenvironmental reconstructions and applied geology.
75 This work shows differences in the geochemical compositions between trace fossils and

their host sediment in an upper Pliensbachian-lower Toarcian marl-limestone rhythmite sequence in the Betic Cordillera of southern Spain.

2. Geological setting

This study was focused on the La Cerradura section, located on a slope along highway A-44 (37º41´47.8´´N; 3º37´57.6´´W), 15 km south of Jaén city (province of Jaén) at km 57. The studied section belongs to the External Subbetic (Fig. 1; Betic External Zones; Reolid et al., 2018). The Betic External Zones comprise the Prebetic and Subbetic, both made up of thick successions of Triassic to Miocene strata (Vera, 2004). The Prebetic sediments were deposited in more proximal settings (shallow marine shelf, coastal plain, and continental environments) during the Jurassic and Cretaceous. The Subbetic represents distal settings, i.e. pelagic swells and subsiding central troughs during the Jurassic. The studied interval ranges from the Algovianum Zone (upper Pliensbachian) to the Polymorphum Zone (lower Toarcian) and comprises hemipelagic marls and marly limestones of the Zegrí Formation. The fragmentation of the south Iberian palaeomargin during the late Pliensbachian and the variable subsidence of different tilted blocks controlled the differences in thickness and facies during the Toarcian (Reolid et al., 2018). In La Cerradura section, the main changes in lithofacies are registered around the Polymorphum/Serpentinum zone boundary (Figs. 1 and 2) related to decreasing carbonate content and the development of dark marls associated with the Toarcian Oceanic Anoxic Event (T-OAE) and a negative carbon isotopic excursion (CIE) (Reolid et al., 2014). The T-OAE has been recognised in the Zegrí Formation (e.g., Jiménez et al., 1996; Rodríguez-Tovar and Reolid, 2013; Reolid, 2014; Reolid et al., 2014) in the Serpentinum Zone. In La Cerradura section, the lower part of

the Serpentinum Zone is also characterised by an increase in total organic carbon (TOC), a negative CIE, and an increase in redox sensitive elements (Reolid et al., 2014; Rodrigues et al., 2019). This succession has low TOC contents (around 0.3 wt.%) with the highest values (0.46 wt.%) around the Polymorphum-Serpentinum zone boundary (Rodrigues et al., 2019). The main contribution to the organic matter content in La Cerradura section is from terrestrial input with a minor marine contribution (see Rodrigues et al., 2019). Trace-fossil assemblage diversity is low in the Serpentinum Zone and, locally, trace fossils are absent in the interval of maximum values of TOC and the negative CIE.

3. Materials and methods

La Cerradura section is 81.6 m thick including upper Pliensbachian and lower Toarcian. Strata with the Algovianum Zone (upper Pliensbachian) through the Polymorphum Zone (lower Toarcian) are composed of alternating marls and marly limestones (65.1 m), whereas the Serpentinum Zone is represented by dark marls (16.5 m). Marly layers of the rhythmite are composed mainly of calcite (average 71%), phyllosilicates (19%), quartz (6%), and minor amount of K feldspar, gypsum, and celestine. Phyllosilicates correspond to illite and illite/smectite mixed layers (average 86%), kaolinite, and chlorite. The amount of calcite in the dark marls of the Serpentinum Zone is lower (53%) than in the rhythmite, whereas phyllosilicates content is higher (35%). This mineralogical composition was also reported by Palomo (1987) from other Pliensbachian and Toarcian sections of the Subbetic.

For this study, a total of 21 samples were collected from the marly limestone beds of the Algovianum (14) and Polymorphum (7) zones. Polished slabs with 1 cm thick were prepared and scanned at the Universidad de Jaén using a Bruker XR-microfluorescence

M4 Tornado equipped with a rhodium target X-ray tube with a high voltage of 50 kV, a current of 600 μA and pressure of 20 mbar. The spotsize of the X-ray optics is 25 μm. The maximum penetration depth from which fluorescence X-rays can still reach the detector is less than 20 μm, which allows for the comparison of the different polished slabs independently of their thickness. This low penetration does not allow deep analysis inside the rock, it does permit analyses of vertical and lateral compositional changes, especially the contrast between the host sediment and the infills of trace fossils.

The geochemical compositional maps obtained for each element are represented by a range of colour intensity that indicates the relative concentration of each element. The microfacies and the burrow infillings were characterised in thin section using a stereographic petrographic microscope Leica M205 C. In addition, carbon-coated polished thin sections were examined by scanning electron microscopy (SEM) using back-scattered electron (BSE) images and energy dispersive X-ray spectroscopy (EDX) with a Merlin Carl Zeiss instrument housed in the Centro de Instrumentación Científico-Técnica of the Universidad de Jaén (Spain). This technique was employed to obtain textural data from BSE imaging based on the atomic-number contrast mode and semi-quantitative chemical data by EDX analysis. Sieved samples were prepared for the Polymorphum Zone for determining the presence of phytodetritus in the < 500 μm fraction. The retrieved small wood fragments were photographed in the SEM with secondary electrons images.

4. Results

Reolid et al. (2014) previously analysed the trace fossil assemblages from the Emaciatum Zone (upper Pliensbachian) to Serpentinum Zone (lower Toarcian) and

identified six ichnogenera. These include common *Planolites*, *Thalassinoides*, *Teichichnus*, and *Chondrites*, and rarer *Palaeophycus* and *Trichichnus*. In addition to these ichnogenera, *Taenidium* and *Lamellaeichnus* were also documented in the Algovianum Zone in the current study (Fig. 3). Most of the ichnogenera corresponds to dwelling structures with passive infilling (*Thalassinoides*, *Teichichnus*, and *Palaeophycus*) and burrows of deposit-feeders with active infilling (*Planolites*, *Lamellaeichnus*, and *Taenidium*) (see Gerard and Bromley, 2008). *Chondrites* has been interpreted as a unknown deposit-feeder tracemaker adapted to oxygen depleted conditions (Savrda and Bottjer, 1986; Fu, 1991) as a chemosymbiotic organism involving sulphide microorganisms (e.g. Ekdale and Bromley, 1984)

Field observations show that the infill of the trace fossils are darker in colour than the host rock both in marls and marly limestone beds (Fig. 3). Such ichnofabrics are referred to as dark-on-light zones by Savrda (2007). In the analysis under the stereographic microscope, the fills of trace fossils also contain higher concentrations of small (< 5 mm) wood fragments (preserved as coal) and pyrite framboids than the host mudstones do (Figs. 4 and 5). Coal fragments are particularly more evident in the samples coming from the Polymorphum Zone (Figs. 3E, F). The semi-quantitative analysis by EDX confirmed that black grains observed in BSE images are organic matter. Moreover, wood remains are identified after the analysis of sieved samples (Fig. 6), and their presence was also reported by Reolid et al. (2019b).

The BSE images of the thin sections (Fig. 5) comprising the burrow fills show the presence of pyrite framboids as previously reported by Gallego-Torres et al. (2015) in the Fuente Vidriera section, also located in the External Subbetic. Pyrite associated to trace fossils may appear as single framboids but commonly as lenticular-shape and dumbbell-

shape polyframboid aggregates. Only locally, pyrite concretions have been identified in areas with high pyrite framboid content.

The compositional maps obtained with the XR-microfluorescence show chemical differences in the content of some elements between the burrow fills and the host sediment (Figs. 7-10). These compositional differences are not uniform within a sample and they can change even within a single trace fossil.

The compositional maps of trace fossils of the Algovianum Zone display a clear enrichment in pyrite framboids as deduced by higher concentrations in Fe and S (Figs. 7 and 8). Pyrite framboids are mainly concentrated in medium- and large-diameter trace fossils such as *Planolites*, *Thalassinoides,* and *Lamellaeichnus* (Figs. 7 and 8). The enrichment in pyrite framboids is less common in smaller trace fossils such as *Chondrites* (Fig. 7). However, the enrichment in Fe and S is less evident in other samples from the Algovianum Zone with the same ichnoassemblage (Fig. 9). Some trace fossil fills also contain higher concentrations of Si, Al, K, Ba, and Cr compared to the host sediment (Fig. 9). However, within a single sample other trace fossils show depletion in Si, Al, and K (Fig. 9).

Trace fossils at the top of the Polymorphum Zone (Fig. 10) are characterised by the same compositional features of those of Algovianun Zone, with an enrichment in pyrite framboids (Fe and S) and minor trace elements such as Cr, Zn, and Ti. The record of large *Chondrites* corresponding to the ichnospecies *Chondrites affinis* requires special consideration. These are characterised by a branched trace fossil with large size (burrow width ranges from 4 to 5 mm) of almost horizontal, flat, straight to slightly curved tunnels (see more details in Uchman et al., 2012). These burrow systems are enriched in organic matter (OM, Fig. 3E) and, locally, iron oxides (Fig. 3F). In the compositional maps, *Ch.*

199 *affinis* show enrichments in Si, Fe, S, Al, K, Ba, Cr, Ti, and Zn (Fig. 10) and a depletion
200 in Ca.
201
202 **5. Discussion**
203
204 The most outstanding characteristic of the studied trace fossils from the limestones
205 of La Cerradura section, is that they are darker than their host sediment. Savrda (2007)
206 interpreted that dark-on-light burrows were passively or actively filled with overlying
207 darker sediment located at the sediment-water interface or mixed layer. However, the
208 colours of marls and limestones comprising the rhythmite of La Cerradura section are
209 approximately the same in fresh samples. The analyses of XRF elemental maps of the
210 burrow fills in La Cerradura section (Figs. 7–10) show that the geochemical and
211 mineralogical compositions in the burrows fills differ from their host sediment.
212
213 *5.1. OM, Fe, and S distribution: Implications for oxygenation degree*
214
215 The bulk enrichment in Fe and S of the burrow fills relative to the host sediments
216 may point to the fact that reducing conditions were preserved in the sediment infilling of
217 the burrows. The presence of pyrite framboids within the burrows observed in the XRF
218 elemental maps (Figs. 7-10) as well as in the BSE images (Fig. 5) is congruent with
219 reducing conditions during the sediment infilling within the burrow. However, it is not
220 possible to infer oxygen depleted conditions at the seafloor at the time of the deposition
221 of the Algovianum and the Polymorphum zones given the abundance and diversity of
222 trace makers that indicate oxygen availability. Buatois and Mángano (2011) proposed that
223 if sediment pore-waters are dysoxic or anoxic, but bottom waters are oxygenated, feeding

traces (fodinichnia) are the dominant ethologic groups, essentially represented by permanent burrow systems that maintain connections to the sediment-water interface. In the studied examples, these reducing conditions are either the result of the location of the burrows under the redox boundary with limited water circulation at the time of their infilling. This sediment infilling may be passive or active. Passive fill results from material entering the burrow gravitationally (more typical of suspension-feeder and predator trace makers such as *Thalassinoides*). Active fill is related to the behaviour of the trace maker such as deposit and detritus feeders (e.g. *Lamellaeichnus*, *Planolites*, *Taenidium*). In the case of *Lamellaeichnus*, the distribution of Fe and S in the sediment infilling the trace (Figs. 7–9) is not homogeneous, indicating that the infilling of burrow tunnels was active and that the distribution of pyrite framboids may be related to faecal origin. Microbially mediated precipitation of Fe minerals related to faecal pellets excreted by a sediment-feeder trace-maker have been documented previously by Izumi et al. (2015) and Harding and Ekdale (2018). Pyritization of fecal pellets and coprolites have been also reported (e.g. Odin et al., 2016; Emmings et al., 2019). According to Simo and Tomasovych (2013), the trace maker of *Lamellaeichnus* was a deposit-feeder that was tolerant of oxygen depleted bottom waters. However, in the studied materials, reducing conditions were only reached beneath the redox boundary within the sediment (Fig. 11).

Pyrite associated to trace fossils occurs as single framboids, lenticular-shape polyframboid aggregates, and dumbbell-shape polyframboid aggregates. These shapes are related to a synsedimentary or earlier hypoxic diagenesis context (Wilkin et al., 1996; Wang et al., 2013). Only locally, pyrite mass concretions have been identified in areas with high pyrite-framboid content interpreted as diagenetic pyrite.

Waslenchuk et al. (1983) studied modern burrow waters of *Callianassa* shrimp characterised by concentrations of nutrients, sulfide, and organic carbon that were higher

than in overlying bottom-waters. These authors proposed the existence of chemical gradients from pore-water to burrow-water affecting remineralised nutrients and trace elements (NH_4^+, NO_2^-, NO, N_2O, Fe^{2+}, S^{2-}, and CH_4). In the case of *Callianassa*, Waslenchuk et al. (1983) measured oxygen-poor, sulfide-rich burrow-water and inferred that *Callianassa* shrimp and associated microbial community were tolerant of oxygen-depleted conditions. Therefore, in the studied examples from the Lower Jurassic, it is proposed that the reducing conditions were developed below the sediment-water interface, but the chemical gradient from pore-water to burrow-water favoured the preservation of OM included in the sediment fills of the burrow passively or actively (faecal pellets?) by the tracemaker (Fig. 12). In general, the vertical distribution of the OM within the sediment presents a gradient. Organic matter is more abundant close to the sediment-water interface (Figs. 11 and 12), which results in a peak of available trophic resources for deposit and detritus feeders that preferentially occupy shallow tiers (Walker and Bambach, 1974; Olóriz et al., 2006; Reolid et al., 2008; Buatois and Mángano, 2011). The OM that accumulated at the seafloor was not preserved due to the oxidation, consumption by benthic organisms and microorganisms, and the subsequent sulfate reduction below the redox boundary within the sediment. The especial environment of the burrows favoured a relatively higher OM matter content due to the infilling by comparatively organic-matter richer sediment derived from the sediment-water interface (also called mixed layer). Thus, the burrows worked as traps for OM preservation (Fig. 12). Remineralization of OM by sulfate-reducing bacteria (SRB) within the burrow fills during the early diagenesis favoured the precipitation of pyrite.

5.2. Enrichment of elements related to detrital input

Some trace fossils from limestone and marly-limestone intervals contain relatively high concentrations of Si, Al, and K with respect to the host sediments, which likely reflects an enrichment of clay minerals in the burrow tunnel (Figs. 9 and 10). This is probably associated with the infilling from overlying marly layers of the rhythmite. In some cases, the trace fossils show enrichment in Cr, Zn, and Ti. Chromium under normal sea-water conditions is soluble as chromate anion (Tribovillard et al., 2006), but under oxygen depleted conditions, Cr(IV) is reduced to Cr(III), forming hydroxyl cations that can be incorporated to humic and fulvic acids. The Cr(III) is not incorporated to Fe-sulfides such as pyrite framboids (Morse and Luther, 1999), and therefore, the remineralization of the OM by SRB does not favour the trapping of Cr within the sediment as sulfide. Thus, the Cr content is related to OM or clay minerals. In the case of Zn, it has a low sensitivity to pyritization (Thomson et al., 1998; Morse and Luther, 1999; Tribovillard et al., 2006). Titanium in sedimentary basins is usually interpreted as related to detrital input (as rutile or substituting in the clay minerals; Spears and Kanaris-Sotiriou, 1976), mainly of eolian origin (Pye, 1987; Chen et al., 2013; Rodríguez-Tovar and Reolid, 2013). For this reason, the enrichment of Zn, Cr, and Ti also could be related to the presence of clay minerals that incorporated these elements. According to Palomo (1987) in coeval sections of the Subbetic, the clays are mainly illite, illite/smectite mixed layers, kaolinite, and chlorite. The enrichment in Ba within some trace fossils describes the same distribution that Si, Al, and K and is interpreted as related to fine detrital plagioclase or barite crystals.

5.3. Sediment infilling of Chondrites affinis*: the potential relation to the T-OAE*

298 The composition of the burrow fills shows the original signal of the redox
299 conditions below the sediment-water interface, which was different to the seafloor where
300 organic matter was consumed and decayed. This higher content of organic matter and the
301 reducing conditions within the burrows favoured the formation of pyrite framboids. The
302 OM enrichment of the sediment infills of trace fossils near the top of Polymorphum Zone,
303 especially in the case of *Chondrites affinis*, may be related to the oxygen-depleted
304 conditions developed in the dark marls of the Serpentinum Zone. These marls have been
305 related to the T-OAE (Reolid et al., 2014; Baeza-Carratalá et al., 2017; Reolid et al.,
306 2019b; Rodrigues et al., 2019). The relative increase of OM (Fig. 3E, F) and Cr (Fig.
307 10H) contents of the *Ch. affinis* could be related to the beginning of the T-OAE in the
308 overlying dark marls of Serpentinum Zone where increased values of TOC and Cr have
309 been reported (Reolid et al., 2014; Rodrigues et al., 2019). The examples of *Ch. affinis*
310 described by Uchman et al. (2012) from the Eocene of the southern Apennines, are also
311 infilled by massive dark mudstones and interpreted as derived from the overlying
312 sediment. A similar situation is observed with the dark mudstones associated with cyclic
313 anoxia in the Oligocene of the Maldives (Swart et al., 2019).
314
315 *5.4. Methodological implications for geochemical sampling of bioturbated rocks*
316
317 The study of oxygen-influenced trace fossils is commonly relevant in the
318 exploration for hydrocarbon resources (Bockelie, 1991; Schieber, 2003; Ekdale et al.,
319 2012). Geochemical analyses of trace fossils exemplified in the current study represent a
320 new ichnological approach that may be of great interest in different research areas
321 included the hydrocarbon exploration. In any case, compositional differences observed

between trace fossils and host rock have relevance for sampling methods of bioturbated sediments when analysing stratigraphic fluctuations of redox geochemical proxies.

The results of this work have implications for the interpretation of geochemical proxies through stratigraphic successions, particularly when elemental analyses are employed to characterise palaeoenvironmental conditions and to predict reservoir quality. Bioturbated rocks may be heterogeneous from geochemical point of view. Hence, careful sampling procedure is needed, except in cases with very low bioturbation and the original sediment fabric is preserved, or where very high bioturbation exists and the fabric is homogeneous. The use of elemental maps is recommended for testing geochemical differences between trace fossils and host rock.

6. Conclusions

Analyses of XRF elemental maps of ichnofossil assemblages from the marl-limestone rhythmite of La Cerradura section (Lower Jurassic, SE Spain) shows that the compositions of the burrow fills are geochemically and mineralogically different with respect to the surrounding sediment. Burrow infills show enrichment in Fe and S relative to the host sediment. This, together with the presence of pyrite framboids within the burrow fills, observed in the XRF elemental maps and in the BSE images, is congruent with reducing conditions. This demonstrates the location of the burrows beneath the redox boundary with low water circulation at the time of their active or passive infilling. This study also shows that reducing conditions acted as traps for organic matter preservation within the burrows, while the organic matter that was accumulated in the seafloor, was not preserved due to oxidation, and consumption by benthic organisms and microorganisms. Thus, the composition of the trace fossil infills reflects different redox

conditions than those at the sediment-water interface. Chemical gradients from pore-water to burrow-water favoured the preservation of OM trapped within the burrow.

The XRF elemental maps also show that some trace fossils from limestone and marly-limestone intervals contain higher concentrations of Si, Al, and K, and other minor components as Zn, Cr, and Ti, with respect to the surrounding host sediment. This is related to the enrichment of clay minerals inside the burrows resulting from infilling from overlying (clastic-richer) marly layer of the rhythmite. Enrichment in Ba within some trace fossils describes the same distribution and may be related to fine detrital plagioclase or barite crystals.

Bulk-rock geochemical analysis should be complemented with elemental imaging of trace fossils in order to evaluate the potential for biogenic heterogeneity and elemental partitioning. Geochemical analysis on trace fossils presented in this work is an implement with respect to classical ichnological work. The compositional differences observed between trace fossils and host rock have relevance for sampling methods employed on bioturbated sediments, particularly for studies directed towards predicting reservoir quality and analysing stratigraphic fluctuations of redox geochemical proxies in palaeoenvironmental studies

Acknowledgments

The MINECO (Spain) is thanked for personal funding to J. Reolid through the Juan de la Cierva Program. This study was supported by the research groups RNM-190 and RNM-200. We wish to thank Prof. Vladimir Simo for identification of the ichnogenus *Lamellaeichnus* and technicians Antonio Piedra and Baltasar Deutor (Universidad de Jaén) for preparing polish slabs and thin sections. We would like to thank Editor Thomas

372 Algeo and two reviewers for their careful supervision of the manuscript. This is a
373 contribution of the IGCP-655 project *Toarcian Oceanic Anoxic Event: Impact on marine*
374 *carbon cycle and ecosystems* (IUGS-UNESCO).

375

376 **References**

377

378 Baeza-Carratalá, J.F., Reolid, M., García Joral, F., 2017. New deep-water brachiopod resilient
379 assemblage from the South-Iberian Palaeomargin (Western Tethys) and its significance for
380 the brachiopod adative strategies around the Early Toarcian Mass Extinction Event. Bulletin
381 of Geosciences 92, 233–256.

382 Bockelie, J.F., 1991. Ichnofabric mapping and interpretation of Jurassic reservoir rocks of the
383 Norwegian North Sea. Palaios 6, 206–215.

384 Buatois, L., Mángano, M.G., 2011. Ichnology: Organism-substrate interactions in space and time.
385 Cambridge University Press, 358 pp.

386 Chen, H.F., Yeh, P.Y., Song, S.R., Hsu, S.V., Yang, T.N., Wang, Y., Chi, Z., Lee, T.Q., Chen,
387 M.T., Zou, J., Chang, Y.P., 2013. The Ti/Al molar ratio as a new proxy for tracing sediment
388 transportation processes and its application in Aeolian events and sea level change in East
389 Asia. Journal of Asian Earth Sciences 73, 31–38.

390 Ekdale, A.A., Bromley, R.G., 1984. Sedimentology and ichnology of the Cretaceous-Tertiary
391 boundary in Denmark: Implications for the causes of the terminal Cretaceous extinction.
392 Journal of Sedimentary Petrology 54, 681–703.

393 Ekdale, A.A., Bromley, R.G., Knaust, D., 2012. The ichnofabric concept. Trace Fossils as
394 Indicators of Sedimentary Environments. Developments in Sedimentology 64, 139–155.

395 Eller, M.G., 1981. The red chalk of Eastern England: a Cretaceous analogue of rosso ammonitico.
396 In: Farinacci, A., Elmi, S., (eds.), Rosso ammonitico symposium proceedings. Tecnocienza,
397 Rome, pp. 233–249.

398 Emmings, J., Hennissen, J.A.I., Stephenson, M.H., Poulton, S.W., Vane, C.H., Davies, S.J., Leng,
399 M.J., Lamb, A., Moss-Hayes, V., 2019. Controls on amorphous organic matter type and
400 sulphurization in a Mississippian black shale. Review of Palaeobotany and Palynology 268,
401 1–18.
402 Fu, S., 1991. Funktion, Verhalten und Einteilung fucoider und lophoctenoider Lebensspuren:
403 Courier Forschungs, Institut Senckenberg 135, 1–79.
404 Fürsich, F.T., 1973. *Thalassinoides* and the origin of nodular limestone in the Corallian Beds
405 (Upper Jurassic) of southern England. Neues Jahrbuch Geologische Paläontologische
406 Abhandlungen 3, 136–156.
407 Fürsich, F.T., 1979. Genesis, environments, and ecology of Jurassic hardgrounds. Neues Jahrbuch
408 Geologische Paläontologische Abhandlungen 158, 1–163.
409 Gallego-Torres, D., Reolid, M., Nieto-Moreno, V., Martínez-Casado, F.J., 2015. Pyrite framboid
410 size distribution as a record for relative variations in sedimentation rate: An example on the
411 Toarcian Oceanic Anoxic Event in Southiberian Palaeomargin. Sedimentary Geology 330,
412 59–73.
413 Gerard, J.R.F., Bromley, R.G., 2008. Ichnofabrics in clastic sediments: applications to
414 sedimentological core studies. Ed. Gerard, Madrid, 100 pp.
415 Gilbert, F., Hulth, S., Grossi, V., Aller, R.C., 2016. Redox oscillation and benthic nitrogen
416 mineralization within burrowed sediments: an experimental simulation at low frequency.
417 Journal of Experimental Marine Biology and Ecology 482, 75–84.
418 Giraldo-Villegas, C.A., Celis, S.A., Rodríguez-Tovar, F.J., Pardo-Trujillo, A., Vallejo-Hincapié,
419 D.F., Trejos-Tamayo, R.A., 2016. Ichnological analysis of the Upper Miocene in the ANH-
420 Tumaco-1-ST-P well: assessing paleoenvironmental conditions at the Tumaco Basin, in the
421 Colombian Pacific. Journal of South American Earth Sciences 71, 41–53.
422 Harazim, D., Mcllroy, D., Edwards, N.P., Wogelius, R.A., Manning, P.L., Poduska, K.M., Layne,
423 G.D., Sokaras, D., Alonso-Mori, R., Bergmann, U., 2015. Bioturbation animals control the
424 mobility of redox-sensitive trace elements in organic-rich mudstone. Geology,
425 doi:10.1130/G37025.1

426 Harding, S.C., Ekdale, A.A., 2018. Trace fossils and glauconitic pellets provide insight into
427 Cambrian siliciclastic marine environments. Palaios 33, 256–265.
428 Izumi, K., 2013. Geochemical composition of faecal pellets as an indicator of deposit-feeding
429 strategies in the trace fossil *Phymatoderma*. Lethaia 46, 496–507.
430 Izumi, K., Rodríguez-Tovar, F.J., Piñuela, L., García-Ramos, J.C., 2014. Substrate-independent
431 feeding mode of the ichnogenus *Phymatoderma* from the Lower Jurassic shelf-sea deposits
432 of central and western Europe. Sedimentary Geology 312, 19–30.
433 Izumi, K., Netto, R.G., Lima, J.H.D., 2015. Microbe-mediated preservation of invertebrate fecal
434 pellets: evidence from the ichnofossil Phymatoderman burkei, Permian shallow-marine,
435 Teresina Formation, Southern Brazil. Palaios 30, 771–778.
436 Jiménez, A.P., Jiménez de Cisneros C, Rivas P, Vera JA (1996) The early Toarcian anoxic event
437 in the westernmost Tethys (Subbetic): Paleogeographic and paleobiogeographic
438 significance. Journal of Geology 104, 399–416.
439 Knaust, D., 1998. Trace fossils and ichnofabrics on the Lower Muschelkalk carbonate ramp
440 (Triassic) of Germany: tool for high-resolution sequence stratigraphy. Geologische
441 Rundschau 87, 21–31.
442 Kristensen, E., 2000. Organic matter diagenesis at the oxic/anoxic interface in coastal marine
443 sediments, with emphasis on the role of burrowing animals. Hydrobiologia 426, 1–24.
444 McBride, E.F., Picard, D.M., 1991. Facies implications of *Trichichnus* and *Chondrites* in
445 turbidites and hemipelagites, Marnoso-arenacea Formation (Miocene), Northern Apennines,
446 Italy. Palaios 6, 281–290.
447 Morse, J.W., Luther, G.W., 1999. Chemical influences on trace metal-sulfide interactions in
448 anoxic sediments. Geochimica et Cosmochimica Acta 63, 3373–3378.
449 Odin, G.P., Belhadj, O., Cabaret, T., Foy, E., Rouchon, V., 2016. Alterations of fossil-bearing
450 shale (Autun, France; Permian), part III: Framboidal pyrite and sulfur as the main cause of
451 efflorescence. Annales de Paleontologie 102, 31–40.

452 Olóriz, F., Reolid, M., Rodríguez-Tovar, F.J., 2006. Approaching trophic structure in Late
453 Jurassic neritic shelves: A western Tethys example from southern Iberia. Earth-Science
454 Reviews 79, 101–139.
455 Palomo, I., 1987. Mineralogía y geoquímica de sedimentos pelágicos del Jurásico inferior de las
456 Cordilleras Béticas (SE de España). PhD Thesis Univ. Granada, 345 pp.
457 Pye, K., 1987. Aeolian dust and dust deposits. Academic Press, San Diego, 334 pp.
458 Reolid, J., Betzler, C., 2018. Ichnofabric logs for the characterization of the organic content in
459 carbonates. Marine and Petroleum Geology 95, 246–254.
460 Reolid, J., Betzler, C., 2019. The ichnology of carbonate drifts. Sedimentology 66, 1427–1448.
461 Reolid, J., Betzler, C., Lüdmann, T., 2019a. The record of Oligocene - Middle Miocene
462 paleoenvironmental changes in a carbonate platform (IODP Exp. 359, Maldives, Indian
463 Ocean). Marine Geology 412, 199–216.
464 Reolid, M., 2014. Stable isotopes on foraminifera and ostracods for interpreting incidence of the
465 Toarcian Oceanic Anoxic Event in Westernmost Tethys: role of water stagnation and
466 productivity. Palaeogeography, Palaeoclimatology, Palaeoecology 395, 77–91.
467 Reolid, M., Nagy, J., Rodríguez-Tovar, F.J., Olóriz, F., 2008. Foraminiferal assemblages as
468 palaeoenvironmental bioindicators in Late Jurassic epicontinental platforms: relation with
469 trophic conditions. Acta Palaeontologica Polonica 53, 705–722.
470 Reolid, M., Mattioli, E., Nieto, L.M., Rodríguez-Tovar, F.J., 2014. The Early Toarcian Ocanic
471 Anoxic Event in the External Subbetic (Southiberian Palaeomargin, Westernmost Tethys):
472 geochemistry, nannofossils and ichnology. Palaeogeography, Palaeoclimatology,
473 Palaeoecology 411, 79–94.
474 Reolid, M., Rivas, P., Rodríguez-Tovar, F.J., 2015. Toarcian ammonitico rosso facies from the
475 South Iberian Paleomargin (Betic Cordillera, southern Spain): palaeoenvironmental
476 reconstruction. Facies 61, 22. Doi:10.1007/s10347-015-0447-3
477 Reolid, M., Molina, J.M., Nieto, L.M., Rodríguez-Tovar, F.J., 2018. External Subbetic Outcrops.
478 In: Toarcian Oceanic Anoxic Event in the South Iberian Palaeomargin. SpringerBriefs in
479 Earth Sciences, pp. 23–83.

480 Reolid, M., Abad, I., Benito, M.I., 2019b. Upper Pliensbachian-Lower Toarcian methane cold
481 seeps interpreted from geochemical and mineralogical characteristics of celestine
482 concretions (South Iberian palaeo-margin). Palaeogeography, Palaeoclimatology,
483 Palaeoecology 530, 15–31.
484 Rodrigues, B., Silva, R., Reolid, M., Mendonça Filho, J.G., Duarte, L.V., 2019. Sedimentary
485 organic matter and $\delta^{13}C_{Kerogen}$ variation on the southern Iberian palaeomargin (Betic
486 Cordillera, SE Spain) during the latest Pliensbachian-Early Toarcian. Palaeogeography,
487 Palaeoclimatology, Palaeoecology 534, 109342.
488 Rodríguez-Tovar, F.J., Reolid, M., 2013. Environmental conditions during the Toarcian Oceanic
489 Anoxic Event (T-OAE) in the westernmost Tethys: influence of the regional context on a
490 global phenomenon. Bulletin of Geosciences 88, 697–712.
491 Rodríguez-Tovar, F.J., Dorador, J., Mayoral, E., Santos, A., 2017. Outcrop and core integrative
492 ichnofabric analysis of Miocene sediments from Lepe, Huelva (SW Spain): Improving
493 depositional and paleoenvironmental interpretations. Sedimentary Geology 349, 62–78.
494 Savrda, C.E., 2007. Trace fossils and marine benthic oxygenation. In: Miller III, W. (ed.), Trace
495 fossil: concepts, problems, prospects. Elsevier, pp. 149–158.
496 Savrda, C.E., Bottjer, D.J., 1986. Trace-fossil model for reconstruction of paleo-oxygenation in
497 bottom waters. Geology 14, 3–6.
498 Schieber, J., 2003. Simple gifts and buried treasures: implications of finding bioturbation and
499 erosion surfaces in black shales. The Sedimentary Record 1, 4–8.
500 Seilacher, A., 1990. Aberration in bivalve evolution related to photo- and chemosymbiosis.
501 Historical Biology 3, 289–311.
502 Simo, V., Tomasovych, A., 2013. Trace-fossil assemblages with a new ichnogenus in “spotter”
503 (Fleckenmergel-Fleckenkalk) deposits: a signature of oxygen-limited benthic communities.
504 Geologica Carpathica 64, 355–374.
505 Spears, D.A., Kanaris-Sotiriou, R., 1976. Titanium in some Carboniferous sediments from Great
506 Britain. Geochimica et Cosmochimica Acta 40, 345–351.

507 Swart, P.K., Blätter, C.L., Nakakuni, M., Mackenzie, G.J., Betzler, C., Eberli, G.P., Reolid, J.,
508 Alonso-García, M., Slagle, A.L., Wright, J.D., Kroon, D., Reijmer, J.J.G., Hui Mee, A.L.,
509 Young, J.R., Álvarez-Zarikian, C.A., Bialik, O.M., Guo, J.A., Haffen, S., Horozal, S., Inoue,
510 M., Jovane, L., Lanci, L., Laya, J.C., Lüdmann, T., Nath, N., Niino, K., Petruny, L.M.,
511 Pratiwi, S.D., Su, X., Sloss, C.R., Yao, Z., 2019. Cyclic anoxia and organic rich carbonate
512 sediments within a drowned carbonate platform linked to Antartic ice volume changes: Late
513 Oligocene-early Miocene Maldives. Earth and Planetary Science Letters 521, 1–13.
514 Thomson, J., Jarvis, I., Green, D.R.H., Green, D., 1998. Oxidation fronts in Madeira Abyssal
515 Plain turbidites: persistence of early diagenetic trace-element enrichments during burial. Site
516 950. Proc. ODP Sci. Results 157, 559–572.
517 Tribovillard, N., Algeo, T., Lyons, T., Riboulleau, A., 2006. Trace metals as paleoredox and
518 paleoproductivity proxies: an update. Chemical Geology 232, 12–32.
519 Uchman, A., Caruso, C., Sonnino, M., 2012. Taxonomic review of *Chondrites affinis* (Sternberg,
520 1833) from Cretaceous-Neogene offshore-deep-sea Tethyan sediments and recommendation
521 for its further use. Rivista Italiana di Paleontologia e Stratigrafia 118, 313–324.
522 Walker, K.R., Bambach, R.K., 1974. Feeding by benthic invertebrates: classification and
523 terminology for paleoecological analysis. Lethaia 7, 67–78.
524 Wang, P., Huang, Y., Wang, C., Feng, Z., Huang, Q., 2013. Pyrite morphology in the first member
525 of the Late Cretaceous Qingshankou Formation, Songliao Basin, Northeast China.
526 Palaeogeography, Palaeoclimatology, Palaeoecology 385, 125–136.
527 Waslenchuk, D.G., Matson, E.A., Zajac, R.N., Dobbs, F.C., Tramontano, J.M., 1983.
528 Geochemistry of burrow waters vented by a bioturbating shrimp in Bermudian sediments.
529 Marine Biology 72, 219–225.
530 Wetzel, A., 2010. Deep-sea ichnology: observations in modern sediments to interpret fossil
531 counterparts. Acta Geologica Polonica 60, 125–138.
532 Wetzel, A., Uchman, A., 2012. Hemipelagic and pelagic basin plains, in: Bromley, R.G., Knaust,
533 D. (Eds.), Trace Fossils as Indicators of Sedimentary Environments. Developments in
534 Sedimentology 64, Elsevier, Amsterdam, pp. 673–701.

Wilkin, R.T., Barnes, H.L., Brantley, S.L., 1996. The size distribution of framboidal pyrite in modern sediments, an indicator of redox conditions. Geochimica et Cosmochimica Acta 60, 3897–3912.

Figure caption

Fig. 1. Location of the studied section. A. Geological setting of the La Cerradura section (star) in the External Subbetic (External Zones of the Betic Cordillera). B. Field view of the outcrop including marl and marly limestone rhythms of the Pliensbachian (Algovianum and Emaciatum zones) and lower Toarcian (Polymorphum Zone), and dark marls of the lower Toarcian (Serpentinum Zone).

Fig. 2. Stratigraphic log of La Cerradura section with location of the studied samples and the interval representing the Toarcian Oceanic Anoxic Event and the negative carbon isotopic excursion (Reolid et al., 2014; Rodrigues et al., 2019).

Fig. 3. Field and polished slab photos of trace fossils. A-D. Ichnoassemblage from Algovianum Zone (upper Pliensbachian). Note: *Ch.*, *Chondrites*; *Th.*, *Thalassinoides*, *Pl.*, *Planolites*, *Ta*., *Taenidium*. E and F. Detail of *Chondrites affinis* from the top of Polymorphum Zone (lower Toarcian) with red circles indicating the presence of organic matter (OM) rich areas. Note the presence of a tunnel composed of iron oxides, probably after pyrite (Py.) in F. Scale bars = 1 cm.

Fig. 4. Trace fossils in thin section. A-D Photomicrographs of *Planolites* under transmitted light (A and C), and reflected light (B and D). Dark particles in A and C are phytodetritus (OM, yellow arrows and circles) and pyrite framboids (Py, white arrows). Pyrite framboids appear as white masses in B. E-F Transmitted light and reflected light images of a *Chondrites affinis*. Pyrite framboids (Py, white arrows) correspond to dark areas in E and to white masses in F.

561 Fig. 5. BSE images of trace fossils in thin section of the Algovianum Zone (upper
562 Pliensbachian). A and B. Lamination within the infilling of *Lamellaeichnus* reflected by
563 the concentration of dark organic particles (OM). Pyrite framboids (Py) appear as intense
564 brightness masses. C. Pyritized section of *Chondrites*. D. Section of partially pyritized
565 unidentified trace fossil.
566 Fig. 6. SEM images of wood fragments preserved as coal retrieved from sieved sample
567 in the Polymorphum Zone.
568 Fig. 7. Polished slab of a burrowed limestone bed from Algovianum Zone (upper
569 Pliensbachian) showing trace fossils (A; yellow areas are weathered parts) and
570 compositional map highlighting the distribution of Fe (B). Abbreviations: *Ch*.,
571 *Chondrites*; *La*., *Lamellaeichnus*; *Ta*., *Taenidium*; *Th*., *Thalassinoides*.
572 Fig. 8. Two polished slabs of bioturbated limestones (A, B) from Algovianum Zone
573 (upper Pliensbachian) and corresponding maps of Fe (C, D) and S (E, F). Note the pyrite
574 concretion in A with 1 cm in diameter. Abbreviations: *Ch*. *Chondrites*; *Pl*., *Planolites*;
575 *Te*., *Teichichnus*; *Th*., *Thalassinoides*; Py., pyrite.
576 Fig. 9. Polished slab of bioturbated limestone (A) from Algovianum Zone (upper
577 Pliensbachian) and corresponding compositional maps for Al, Ba, Cr, Fe, K, S and Si.
578 Some trace fossils observed in A such as *Planolites* (*Pl*.) present enrichment in all
579 elements, others such as *Thalassinoides* (*Th*.) show relative enrichment just for Fe and S
580 but not always, and *Palaeophycus* (*Pa*.) are similar to host sediment.
581 Fig. 10. Bioturbated limestone sample from the top of the Polymorphum Zone (lower
582 Toarcian) and corresponding compositional maps for Si, Ca, Fe, Al, K, Ba, Cr, Ti and Zn.
583 The surface of the sample is parallel to the bedding.
584 Fig. 11 Location of food resources with respect to the sediment-water interface and the
585 idealized vertical distribution of oxic, suboxic, and the reduced zones of Kristensen

586 (2000) compared with the trace-fossil tiering for La Cerradura section. Note: 1) The
587 highest concentrations of OM occur at sediment-water interface; 2) Labile OM is
588 consumed (aerobic respiration and OM oxidation) in the oxic zone within the sediment;
589 3) OM content decreases with depth in the suboxic zone as a result of microbial
590 decomposition by anaerobic bacteria; 4) The microbial activity (mainly SRB, see text)
591 and the labile OM are low in the reduced zone (anoxic conditions) and most of the OM is
592 refractory not a food resource.
593 Fig. 12. Model of OM and oxygen distribution in a transect without burrow (left) and a
594 transect through a burrow (right). Note the vertical distribution of the OM within the
595 sediment presents a gradient with higher content close to the sediment-water interface.
596 OM contents in the seafloor decrease with depth due to consumption by deposit and
597 detritus feeder and aerobic and anaerobic microbial decomposition. However, the burrow
598 contains a comparatively higher OM concentration with respect to the host sediment
599 because it is infilled by material coming from the seafloor. The oxygen-poor, sulfide-rich,
600 burrow-water led to enhanced OM preservation compared with the oxic bottom-waters.
601 In this sense, the burrows served as traps for OM preservation.

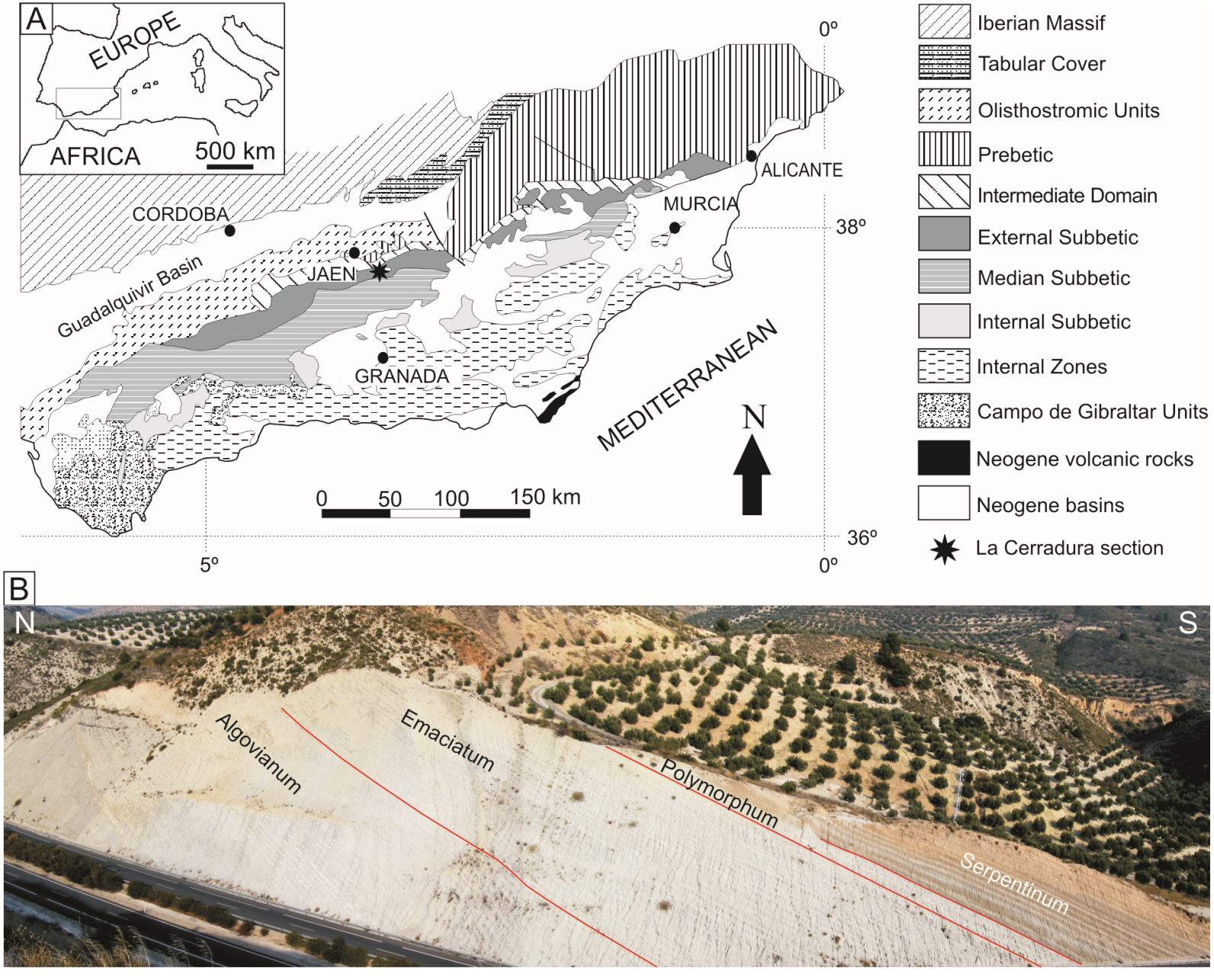
A
EUROPE
AFRICA
500 km
CORDOBA
JAEN
Guadalquivir Basin
GRANADA
ALICANTE
MURCIA
MEDITERRANEAN
N
0 50 100 150 km
0º
38º
36º
5º
0º
Iberian Massif
Tabular Cover
Olisthostromic Units
Prebetic
Intermediate Domain
External Subbetic
Median Subbetic
Internal Subbetic
Internal Zones
Campo de Gibraltar Units
Neogene volcanic rocks
Neogene basins
La Cerradura section
B
N
S
Algovianum
Emaciatum
Polymorphum
Serpentinum

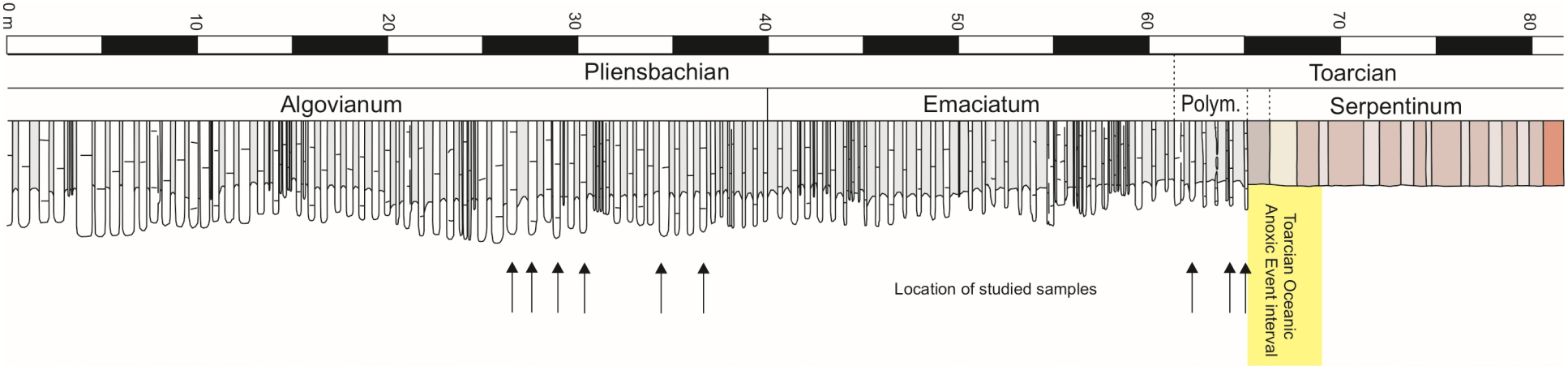
0 m
10
20
30
40
50
60
70
80
Pliensbachian
Toarcian
Algovianum
Emaciatum
Polym.
Serpentinum
Toarcian Oceanic Anoxic Event interval
Location of studied samples

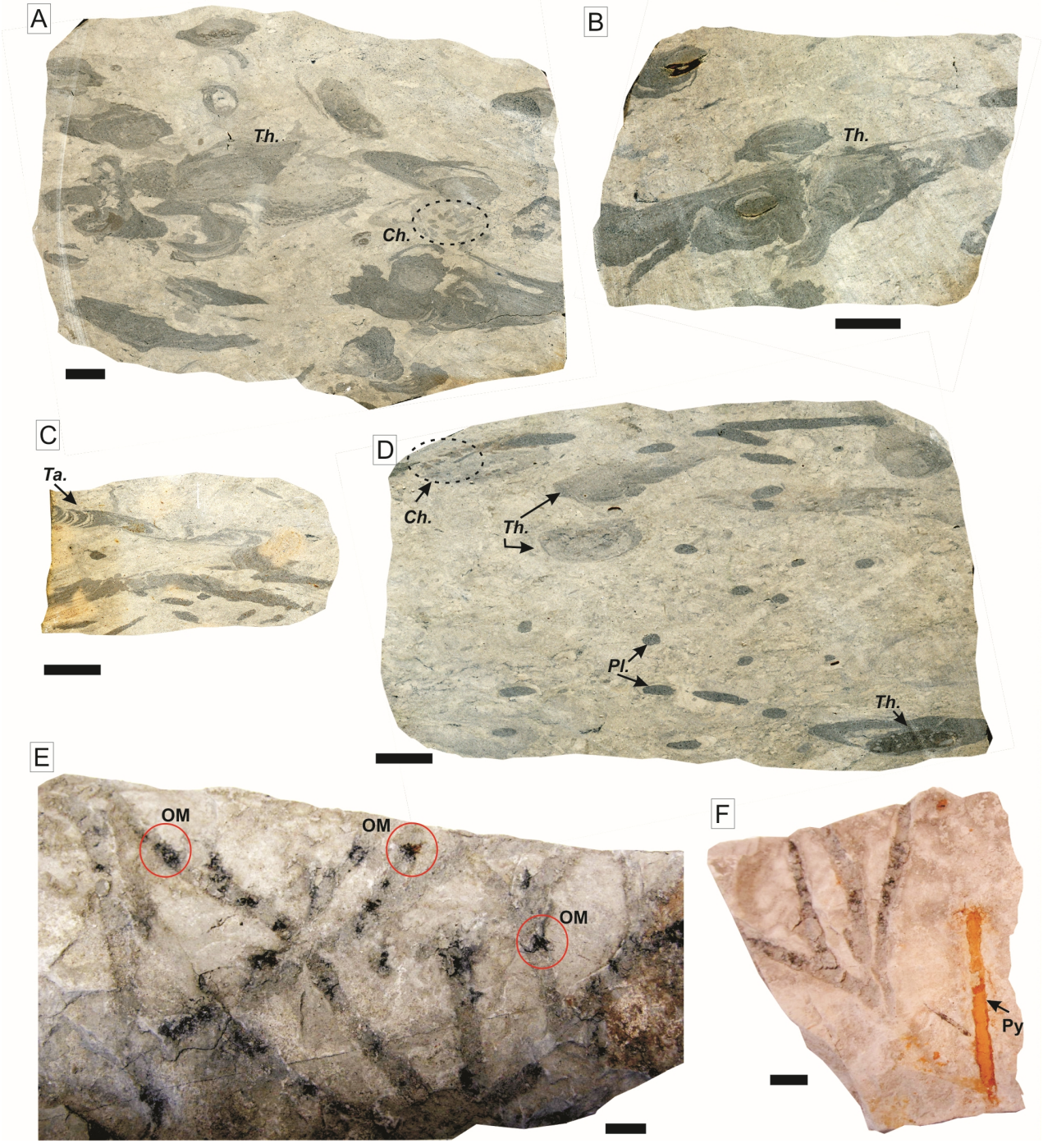
A
Th.
Ch.
B
Th.
C
Ta.
D
Ch.
Th.
Pl.
Th.
E
OM
OM
OM
F
Py

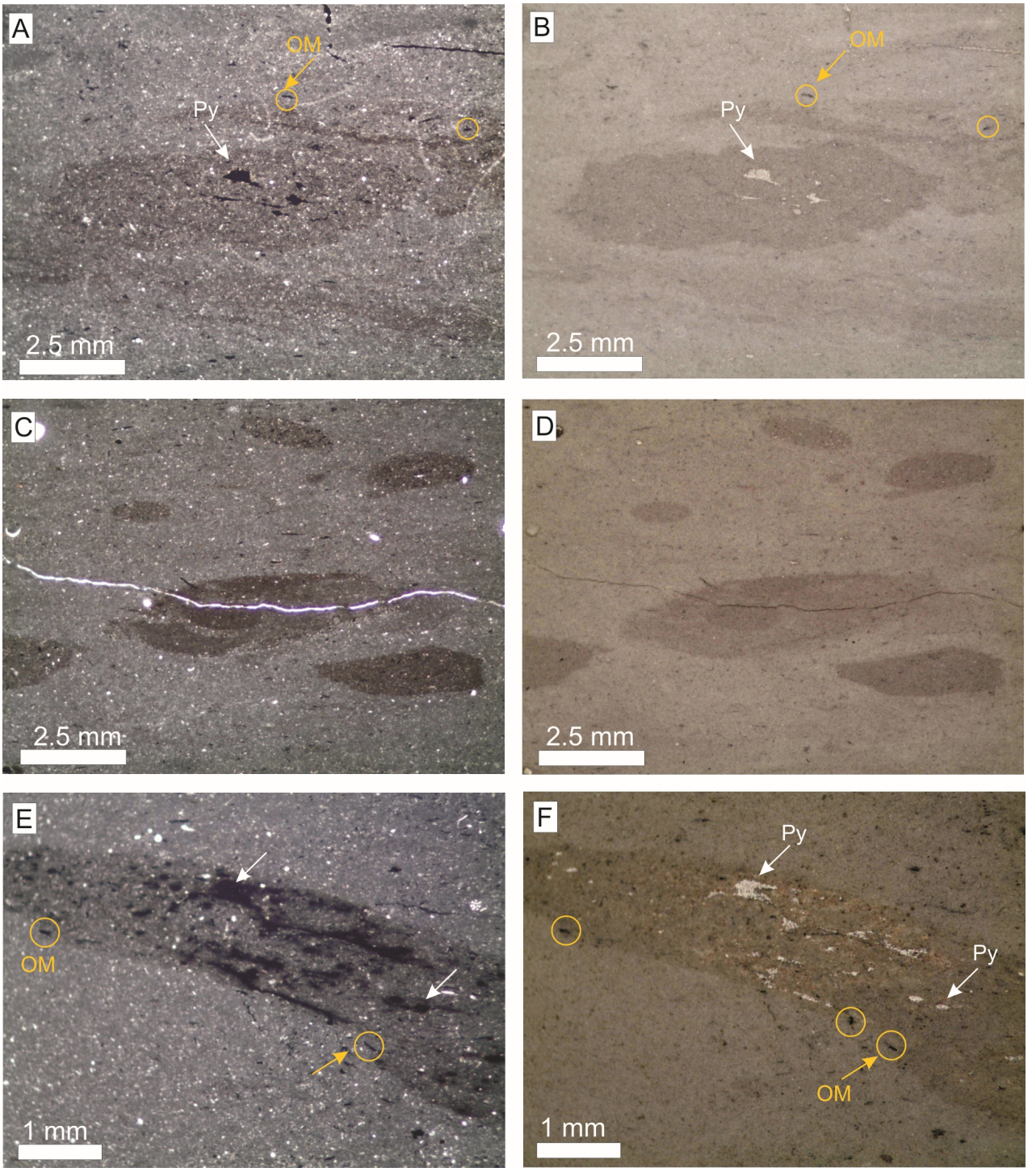
A
OM
Py
2.5 mm
B
OM
Py
2.5 mm
C
2.5 mm
D
2.5 mm
E
OM
1 mm
F
Py
Py
OM
1 mm

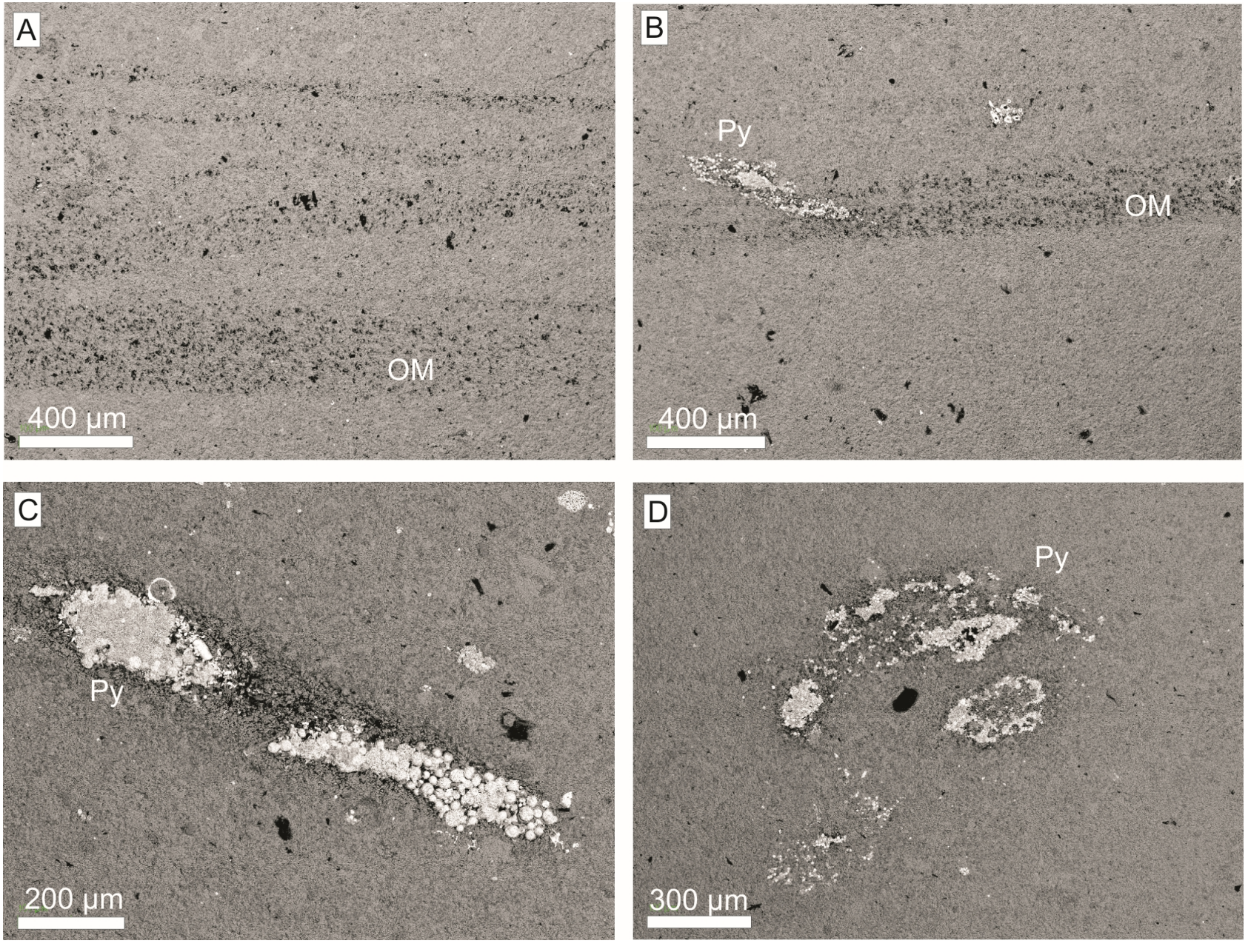
A
OM
400 μm
B
Py
OM
400 μm
C
Py
200 μm
D
Py
300 μm

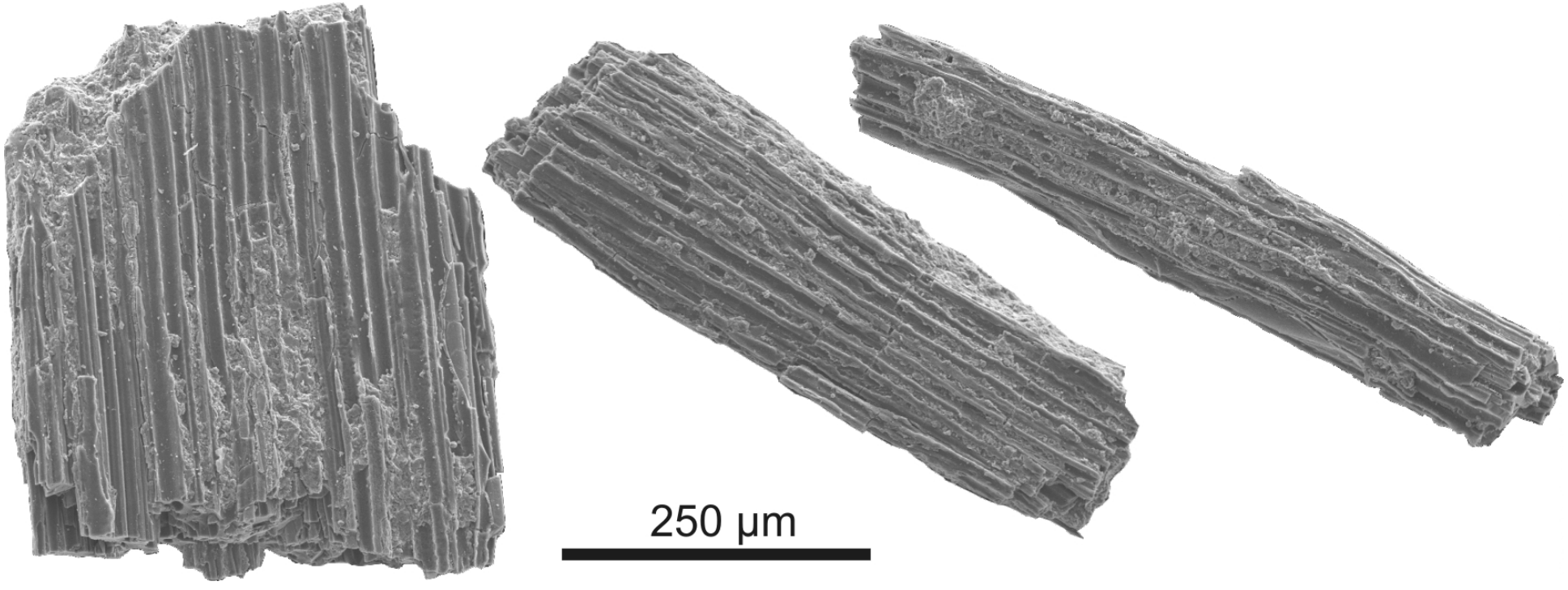
250 µm

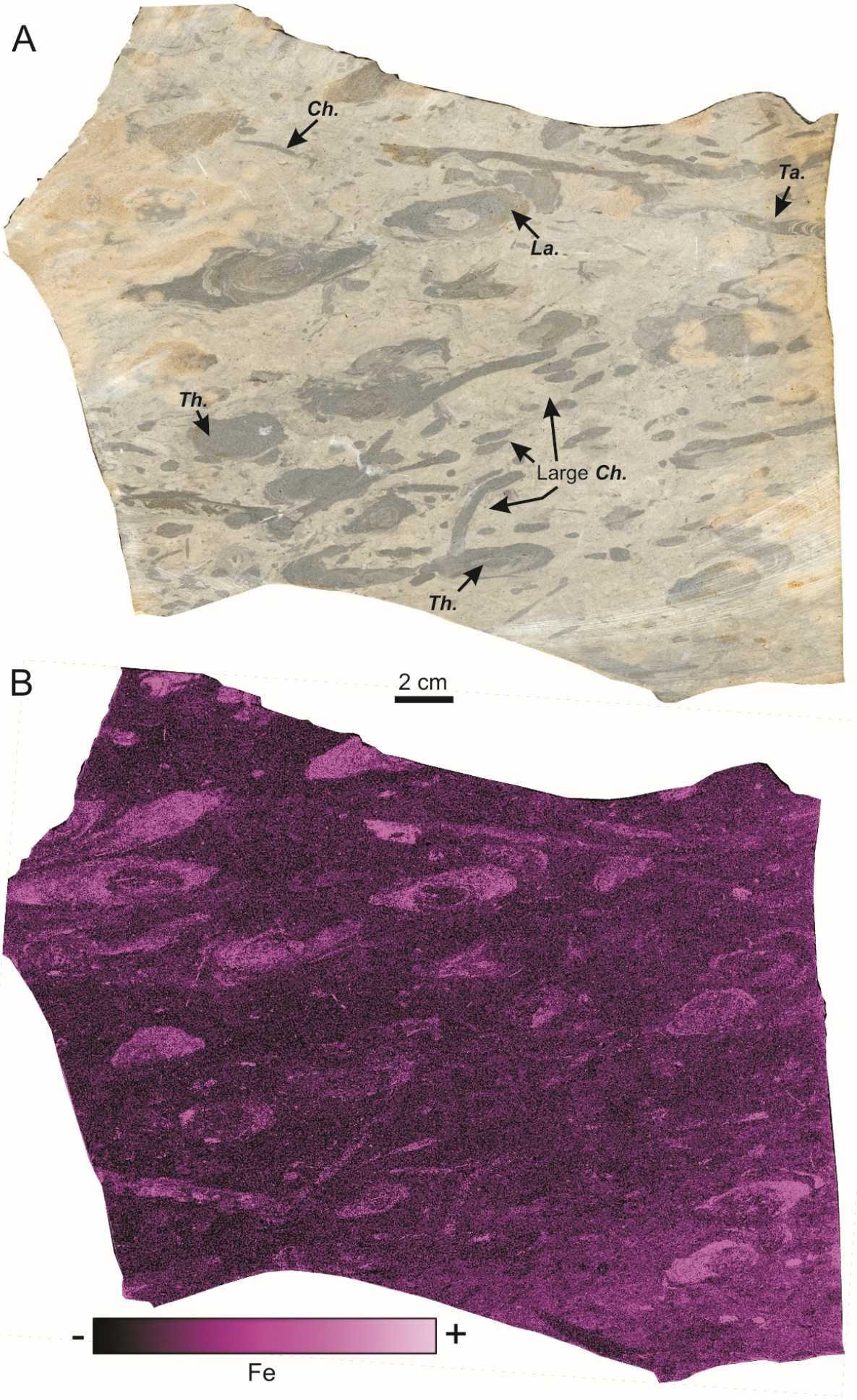
A
Ch.
Ta.
La.
Th.
Large Ch.
Th.
B
2 cm
-
+
Fe

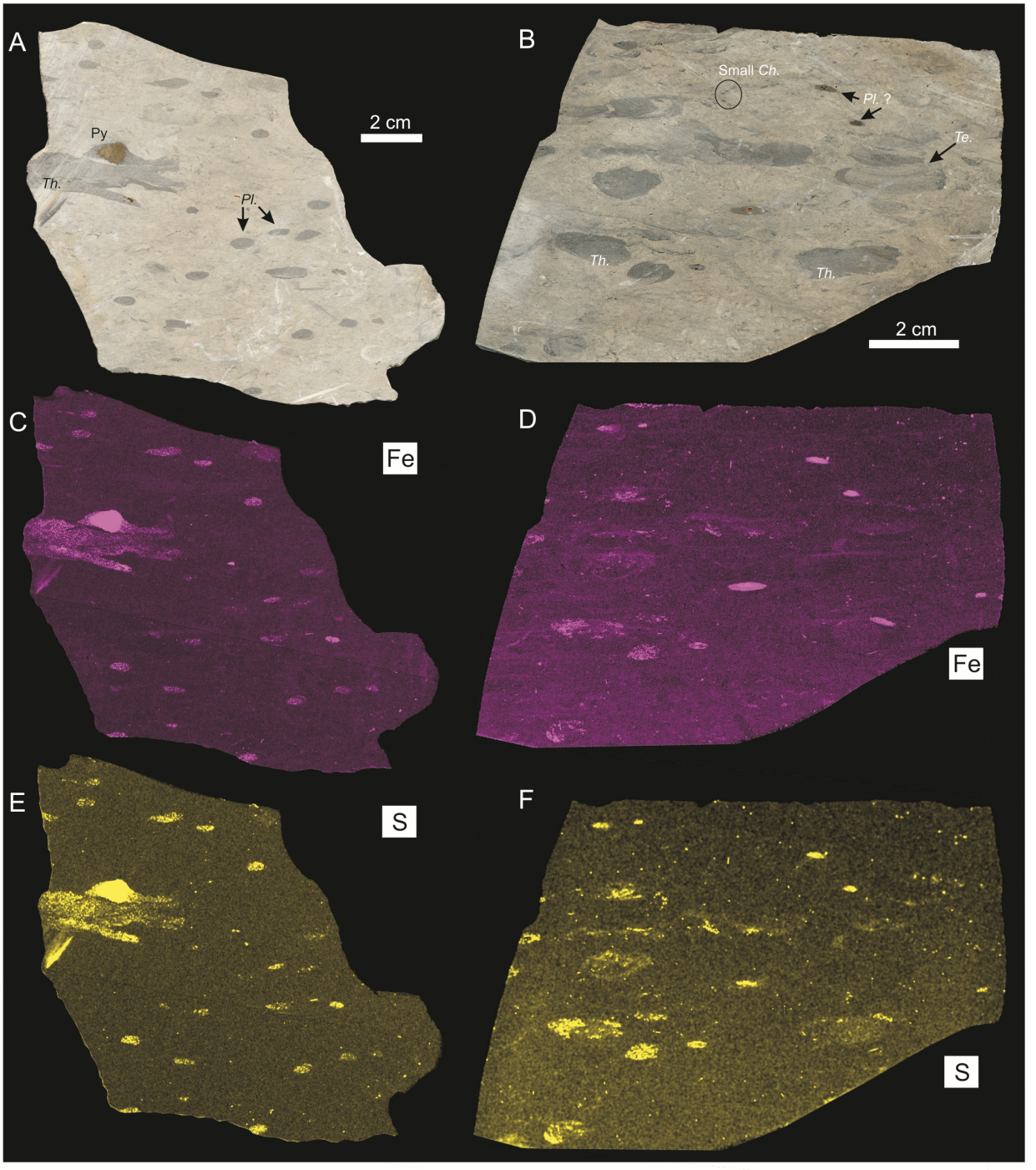
A
Py
Th.
Pl.
2 cm
B
Small Ch.
Pl.?
Te.
Th.
Th.
2 cm
C
Fe
D
Fe
E
S
F
S

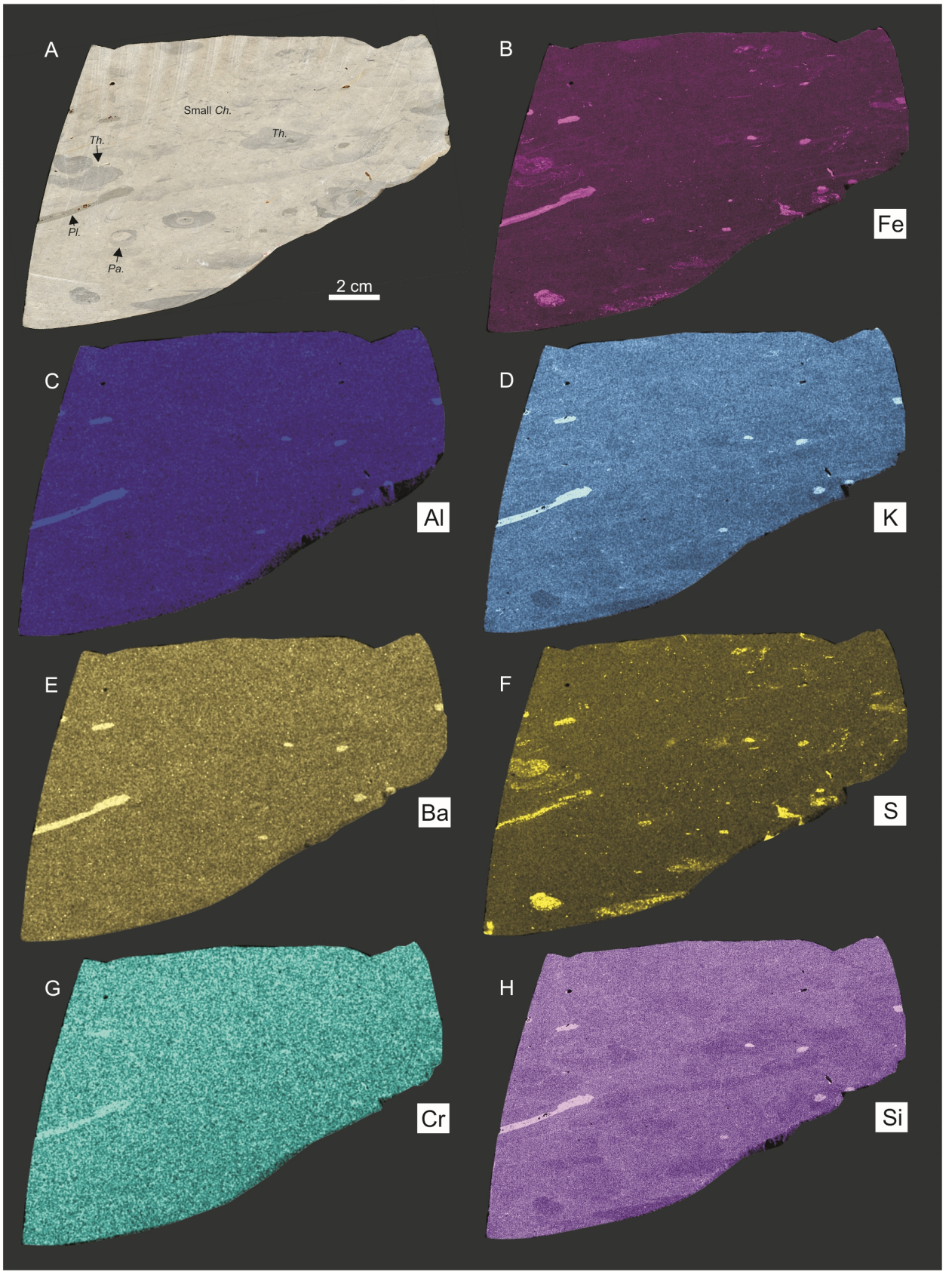
A
Small Ch.
Th.
Th.
Pl.
Pa.
2 cm
B
Fe
C
Al
D
K
E
Ba
F
S
G
Cr
H
Si

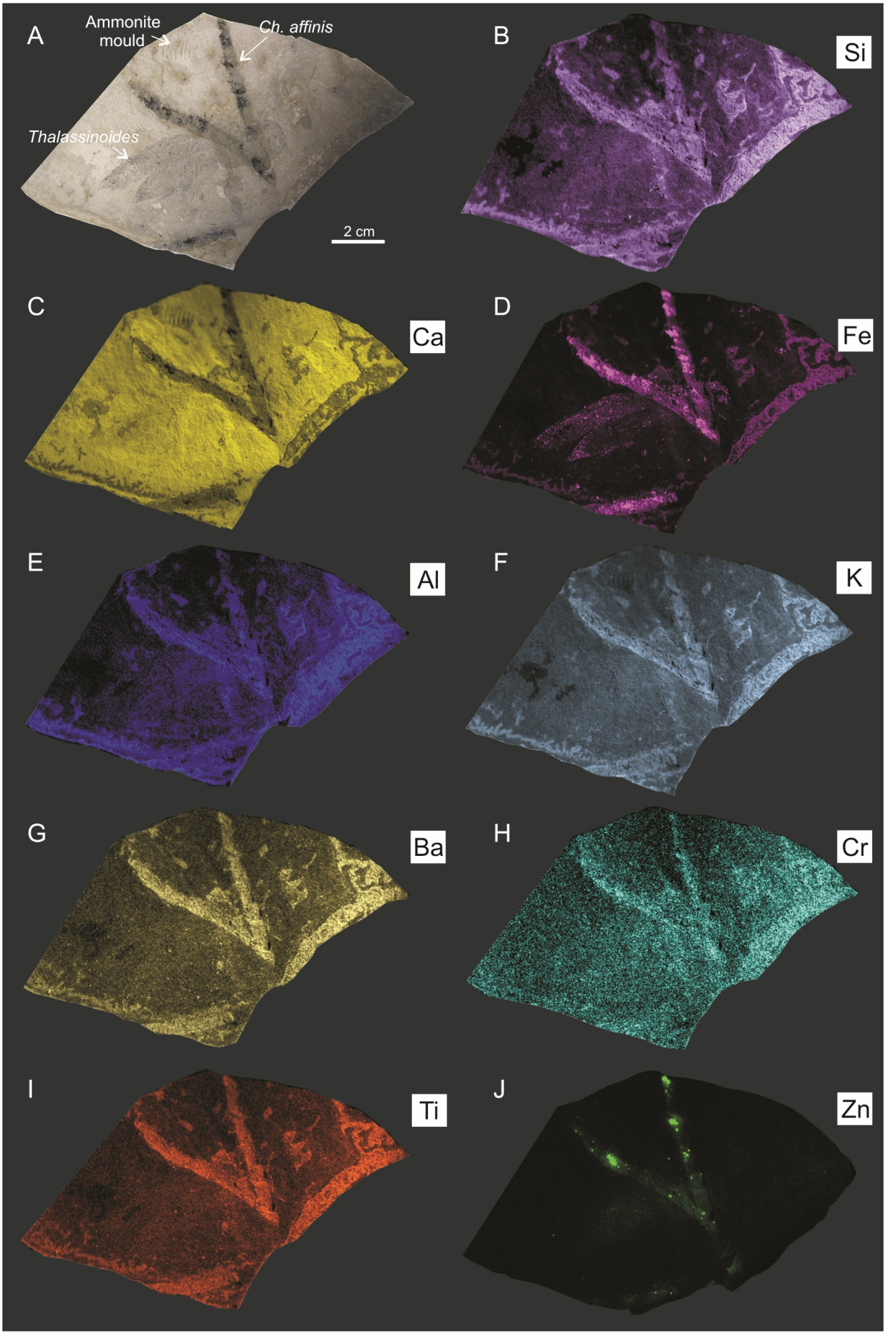
A
Ammonite mould
Ch. affinis
Thalassinoides
2 cm
B
Si
C
Ca
D
Fe
E
Al
F
K
G
Ba
H
Cr
I
Ti
J
Zn

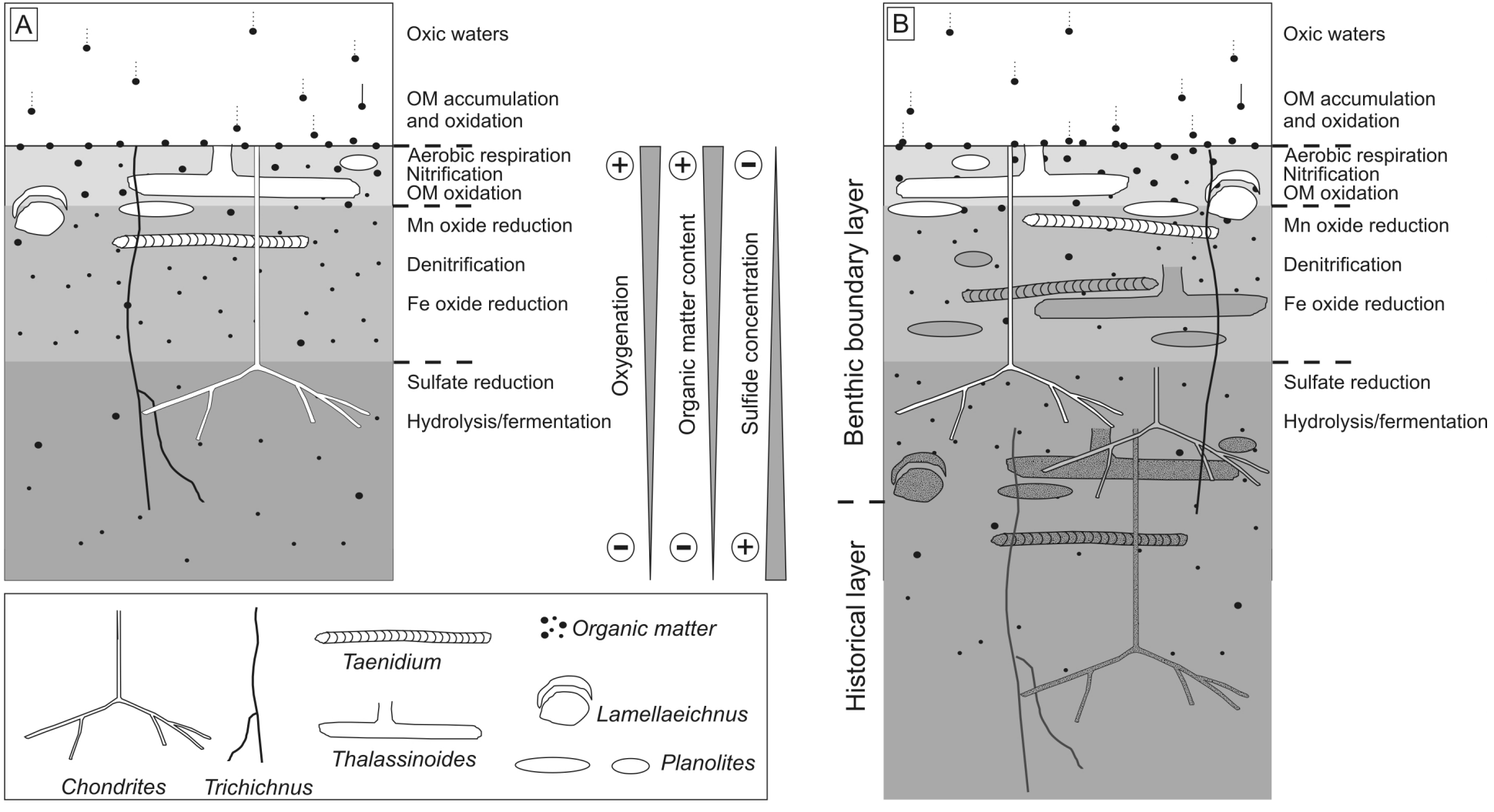
A
Oxic waters
OM accumulation and oxidation
Aerobic respiration
Nitrification
OM oxidation
Mn oxide reduction
Denitrification
Fe oxide reduction
Sulfate reduction
Hydrolysis/fermentation
Oxygenation
Organic matter content
Sulfide concentration
Chondrites
Trichichnus
Taenidium
Thalassinoides
Organic matter
Lamellaeichnus
Planolites
B
Oxic waters
OM accumulation and oxidation
Aerobic respiration
Nitrification
OM oxidation
Mn oxide reduction
Denitrification
Fe oxide reduction
Sulfate reduction
Hydrolysis/fermentation
Benthic boundary layer
Historical layer

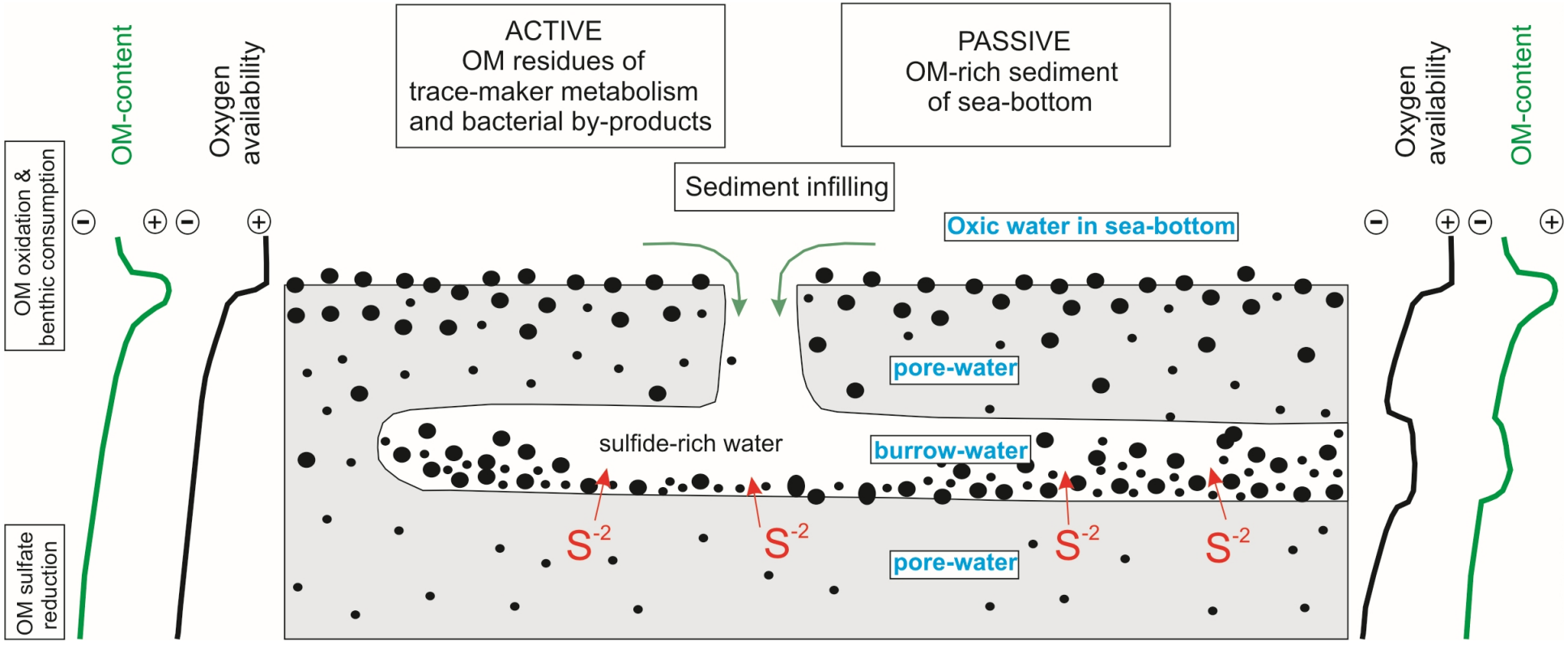
ACTIVE
OM residues of
trace-maker metabolism
and bacterial by-products
PASSIVE
OM-rich sediment
of sea-bottom
OM-content
Oxygen
availability
Sediment infilling
Oxic water in sea-bottom
OM oxidation &
benthic consumption
pore-water
sulfide-rich water
burrow-water
S-2
S-2
S-2
S-2
pore-water
OM sulfate
reduction
Oxygen
availability
OM-content